

Sputtered AlN Thin Films on Si and Electrodes for MEMS Resonators: Relationship Between Surface Quality Microstructure and Film Properties

S. Mishin, D. R. Marx and B. Sylvia,
Advanced Modular Sputtering, Inc,
93 S. La Patera Lane, Goleta, CA 93117

V. Lughi, K. L. Turner, and D. R. Clarke
Materials Department
University of California Santa Barbara
Santa Barbara, CA 93106

Abstract – Aluminum nitride thin films grown by reactive AC magnetron sputtering are characterized using several metrology techniques to examine the correlation between surface quality, microstructure and piezoelectric properties. Atomic force microscopy, X-ray diffraction and electron microscopy, and are employed to characterize the microstructure. A range of substrate coatings is explored to understand the impact of topography on film crystallinity and piezoelectric performance. A first order approximation model providing the piezoelectric characteristics as a function of the c-axis misorientation in the mosaic-structured wurtzite AlN films is presented. While the model predicts a only small $e_{33,eff}$ and kt change for a misorientation distribution of FWHM of less than 5 degrees, it services as a indication of the impact of AlN crystallinity on film piezoelectric properties.

I. INTRODUCTION

As cell phone technology goes to higher and higher frequencies and the MEMS market seeks to put greater functionality into their systems, the need for high quality piezoelectric aluminum nitride, AlN, is growing. With different applications and device designs, a wide range of substrate materials are being considered. These range from Si, or GaAs wafers, wafers coated with poly silicon, SiO₂ (thermal or PECVD) Si₃N₄, and sputtered Mo, Al alloys, Pt, W/Ti and W over these coatings. One measure of the quality of AlN is its crystallinity as measured by the full wave-half maximum (FWHM) values from an XRD rocking curve experiment.

As indicated by Ruby [1], for good piezoelectric properties, AlN crystals must grow in columns that are perpendicular to the plane of the electrodes and in order to achieve this, the surface should be a smooth, “mirror-like” surface otherwise the many facets of a rough surface initiate crystal growth in a variety of directions.

A study has been undertaken in an attempt to evaluate how the underlying surface morphology affects the AlN crystallinity. Using polished prime Si wafers as the benchmark, comparison of structure, are made and correlations to piezoelectric performance will be offered.

II. EXPERIMENTAL

Prime (100) Si wafers were used as the standard substrate. Oxide coatings were either thermally grown or deposited using PECVD methods. Si₃N₄ coatings were also deposited by PECVD. With the exception of Mo, metal electrodes were sputter deposited using DC magnetron sputtering. Mo was deposited using an AC magnetron process.

All AlN films were reactively deposited using an Advanced Modular Sputtering, Inc, AMS 2003 cluster tool utilizing a dual-ring target configuration and employing AC rectification between the rings so as to assure plasma stability and to eliminate issues associated with the “disappearing anode effect”.

III. RESULTS

As a baseline, deposition of AlN directly on prime silicon wafers with high quality low roughness substrate (less than 0.5nm) surface is used. Figure 1 shows the impact of film thickness on the XRD rocking curves. In the range typically used for BAW/FBAR and MEMS applications, values less than 2.0° is achieved.

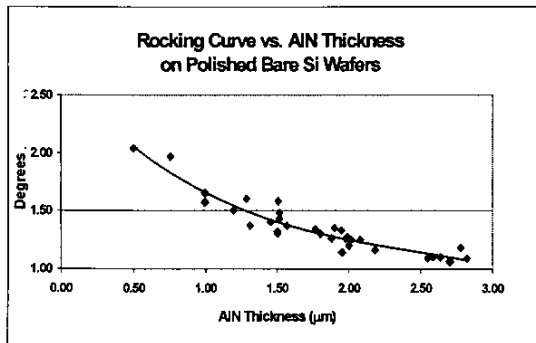


Figure 1. XRD Rocking curve FWHM versus AlN film thickness

The surface roughness, or topography, tends to increase as wafers are coated without any polishing. Figure 2 illustrates the increase in the FWHM values with the addition of a Mo electrode underlayer.

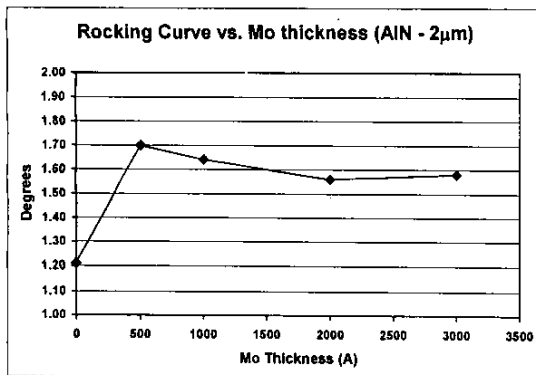


Figure 2. Impact of Mo underlayer on AlN rocking curve.

With Si wafers, coatings of thermal oxide, PECVD oxide and Si_3N_4 are compared, Figure 3. Substrate surface roughness was measured using AFM. If done properly, thermal oxide growth does not significantly change the surface roughness as compared to a prime Si wafer. The PECVD coating is considerably rougher than the thermal oxide and results in a

considerably worse rocking curve. While the AFM micrographs of the prime Si and the thermal oxide are featureless, the roughness of the as-deposited PECVD oxide and Si_3N_4 is clearly observed.

Table 1. Dielectric coatings on Si wafers

	Prime Si	0.8 μm Thermal Oxide	0.8 μm PECVD Oxide	Si_3N_4
Surface Roughness Ra (nm)				
As received	0.207	0.178	4.5	7.8
After CMP			1.3	0.5
XRD FWHM (degrees)				
2.05 μm AlN	1.27	1.23	6.2	

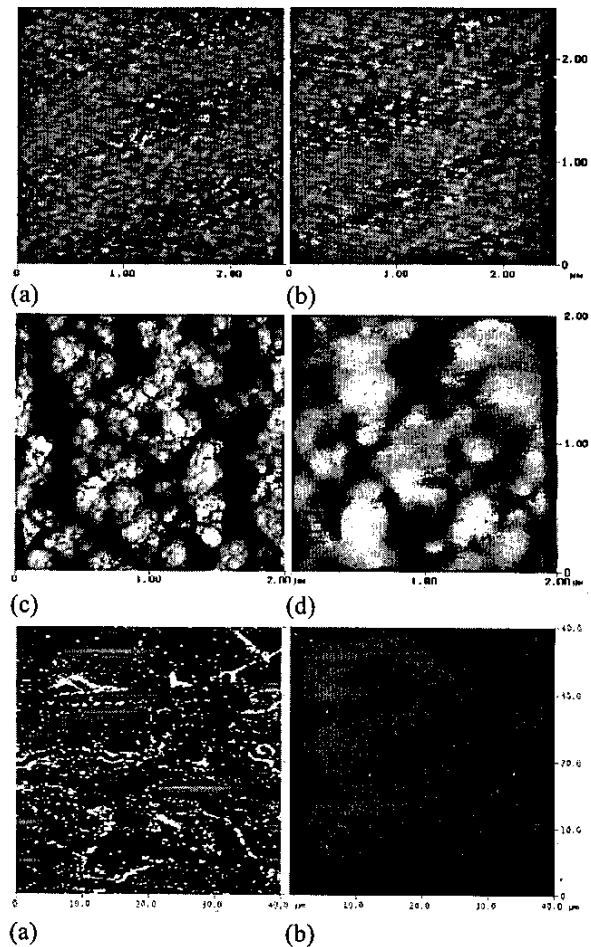


Figure 3. AFMs of substrates (a) prime Si, (b) thermal oxide, (c) PECVD oxide, (d) PECVD oxide after CMP, (e) Si_3N_4 , (f) Si_3N_4 after CMP. Note Figures e and f are at lower magnification.

Metal electrode films are deposited on various coatings. In this evaluation, Mo (200 to 250nm), Al/0.5Cu (180nm)/Ti (20nm), AlSi (200nm) and TiW (200nm) films were considered. Tables 2 and 3 show the surface roughness and the FWHM results after AlN deposition, respectively. With the Mo electrode, it is necessary to provide a barrier between the metal and the substrate to avoid interaction. Without a barrier, the result of the interaction is seen in the large 10° FWHM values.

Table 2. Surface roughness of several electrode materials

	Prime Si	0.8 μm Thermal Oxide	0.8 μm PECVD Oxide w/o CMP	0.8 μm PECVD Oxide with CMP	Si3N4 w/o CMP	Si3N4 with CMP
	Roughness (nm)					
	0.2	0.2	2.8	2.8	7.8	0.5
W/Ti10	2.3		4.3			
AlSi	2.1	2.7	4.1			
Warm AlCu/Ti	1.5	1.2	6.7			
Cold AlCu/Ti	0.7	0.6	2.8	1.3		

Table 3. FWHM of AlN on electrode materials

	Prime Si	0.8 μm Thermal Oxide	0.8 μm PECVD Oxide w/o CMP	0.8 μm PECVD Oxide with CMP	Si3N4 w/o CMP	Si3N4 with CMP
	FWHM (degrees)					
AlN on Mo		10.0	6.4			
AlN on Mo on barrier	1.6	1.5			2.5	1.5
AlN on W/Ti10	14.0		22.0			
AlN on AlSi	7.6		6.4			
AlN on Warm AlCu/Ti	2.0	1.3	5.8	2.3		
AlN on Cold AlCu/Ti	1.7	1.3	2.9	1.9		

A summary of all data collected is shown in Figure 4. While the data scatter is large the general trend is that FWHM decreases as a function of substrate surface roughness. It is observed the high surface roughness, of W/Ti, Figure 5, results in very poor crystallinity independent of the substrate material.

Excellent crystallinity is observed for the AlN deposited on Mo electrodes on Si, thermal oxide and Si3N4 when a barrier layer is employed. Without polishing the AlN crystallinity is poor due to the high

surface roughness. While potentially not the best electrode material due to its acoustic softness, room temperature deposited (cold) AlCu/Ti electrodes on Si exhibited a fairly smooth surface on to which highly crystalline AlN could be grown. Warm deposition of AlCu/Ti produced films with large grains structures. AlCu/Ti on PECVD this resulted in poor crystallinity

FWHM versus Surface Roughness

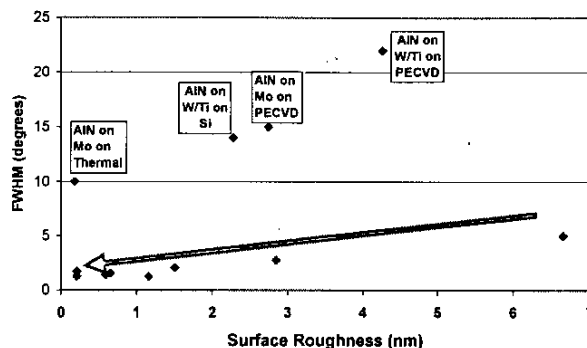


Figure 4. Summary of surface roughness versus XRD FWHM

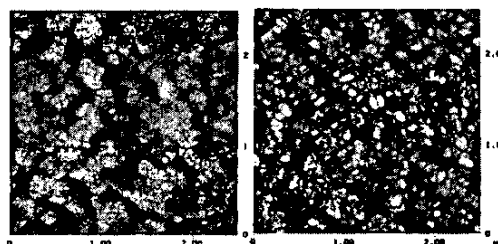


Figure 5. AFM of W/Ti on Si (left) and PECVD oxide (right)

The appearance of resulting AlN films are illustrated in Figure 6. A fine uniform structure is observed for the AlN on Mo and on the cold deposited AlCu/Ti on Si. A less uniform structure is observed when the cold AlCu/Ti is deposited on PECVD oxide. A much less uniform AlN structure is seen for the AlN on W/Ti. The underlying grains structure is clearly seen for the AlN on the warm AlCu/Ti on Si and a highly irregular, non-uniform appearance is observed for the warm AlCu/Ti on PECVD oxide.

Both PECVD oxide and Si3N4 are important to the fabrication of FBAR and MEMS structures. To employ these materials, polishing is needed to produce a smooth surface that, in turn, will provide improved AlN rocking curve results. With Si3N4,

FWHM values decreased from 2.5° down to an acceptable 1.5° . FWHM values dropped to less than 2.3° for polished PECVD for both cold and warm AlCu/Ti.

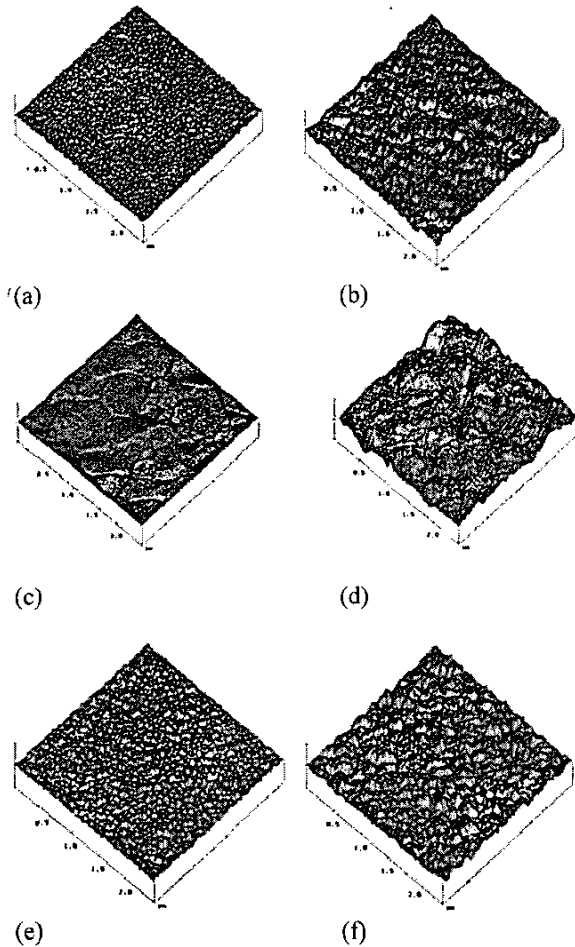
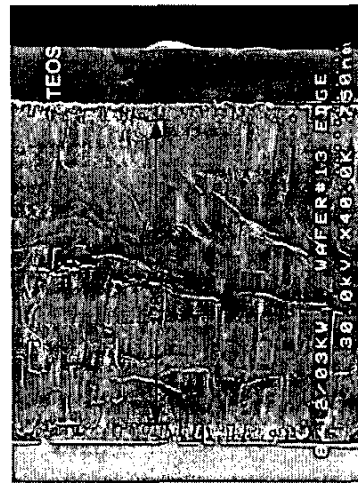


Figure 6. Clockwise from upper left, (a) AlN surface structure deposited on Mo on prime Si, (b) AlN on W/Ti on prime Si, (c) AlN on warm AlCu/Ti on Si, (d) AlN on warm AlCu/Ti on PECVD oxide, (e) AlN on cold AlCu/Ti on Si, (f) AlN on cold AlCu/Ti on PECVD oxide.

IV. DISCUSSION

When an optimized smooth surface structure is provided highly, crystalline AlN can be grown. The high quality film exhibits a fracture surface showing a dense columnar structure as seen in Figure 7.

At higher magnification, Figure 8, TEM examination reveals contrasts between a high and low quality film. The former shows the development of the dense



structure grown on a highly planar Mo electrode surface

column throughout the structure while the poor quality film tends to develop the well-defined columnar structure on a region of less well-defined material.

Figure 7. Fracture surface of a high quality AlN/electrode film stack showing highly columnar



Figure 8. TEM micrographs of high (left) and low (right) quality AlN films.

In a thin film, the effective value of the piezoelectric constants depends on the microstructure of the material. For FBAR geometries, the pertinent constant is $e_{33,eff}$, where the "3" direction is intended to be the direction perpendicular to the free surface of the film. In order to estimate $e_{33,eff}$, we schematize a thin layer of AlN as shown in Figure 9.

This model resembles the typical highly textured microstructure of sputtered AlN, shown in Figure 8.

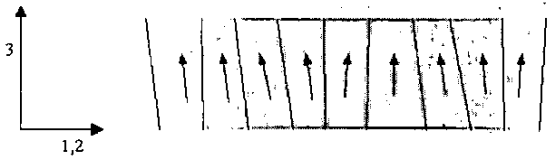


Figure 9. Schematic of a cross section of a typical thin film of sputtered AlN. The arrows represent the direction of the c-axis of each grain. Direction "3" is taken to be perpendicular to the free surface of the film.

The grains are needle-shaped with the long axis – coincident with the wurtzite [0001] axis – preferentially oriented approximately along the growth direction. Considering the piezoelectric contribution of each individual grain along the "3" direction and taking the summation weighted by a Gaussian distribution of the grains' misorientation, we find the result shown in Figure 10 where the effective piezoelectric effect is represented as the ratio between the calculated value and single crystal value a function of the distribution's FWHM. The values for the piezoelectric tensor were taken from Nye [2].

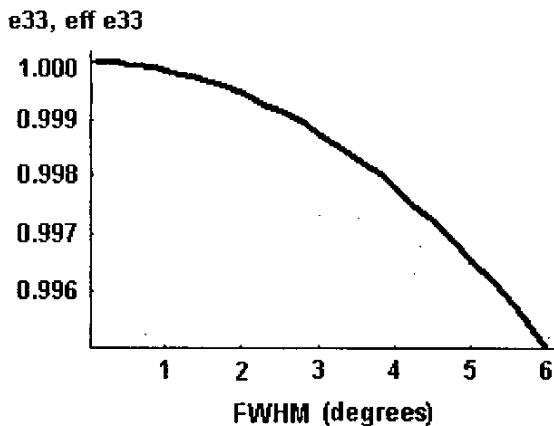


Figure 10. Results of the calculation outlined in the text. It is shown that for a distribution FWHM of approximately 6°, the effective piezoelectric coefficient drops by less than 0.5% of the original value.

It is observed that the effective piezoelectric effect does not change significantly even for grain orientation distributions with FWHM values up to several degrees. Data from Lobl, et al [4], supports contention.

While the model presented here is necessarily simplistic in the sense that all interactions among grains have been neglected, nevertheless, it helps to estimate, to a first approximation, the influence of microstructure on the piezoelectric properties of the thin film

V. CONCLUSIONS

Obtaining high quality AlN films on different electrode materials is a function of the surface quality and to a much lesser extent on the nature of the material. Polishing using CMP techniques provides an excellent avenue to develop a mirror like surface eliminating nucleation sites that may allow growth in directions not perpendicular to the electrode surface.

The UCSB authors acknowledge the support of the US Navy-MINT grant #N66001-01-1-8965

VI. REFERENCES

- [1] R. Ruby, "Cavity spanning bottom electrode of a substrate-mounted bulk acoustic wave resonator." US Patent No.6,384,697, May 7, 2002.
- [2] J. F. Nye, Physical Properties of Crystals: Their Representation by Tensors and Matrices.: Oxford University Press, Oxford 1985.
- [3] A.Gualtieri and J.G. Ballato, "Piezoelectric Materials for Acoustic Wave Applications." IEEE Transactions on Ultrasonics, Ferroelectrics and Frequency Control, vol. 41, pp 53-59, January 1994.
- [4] .H.P.Lobl, M.Klee, C. Metzmacher, W.Brand, R. Milsom, P.Lok, F.van Straten "Piezoelectric materials for BAW resonator and filters", 2001 IEEE International Ultrasonics Symposium, Atlanta, GA, Oct. 7-10, 2001, paper 3E-2, pp. 807-811.